Bulletin of Environment, Pharmacology and Life Sciences
Bull. Env. Pharmacol. Life Sci., Vol 9[4] March 2020 : 66-73

Online ISSN 2277-1808
Journal's URL:http://www.bepls.com
CODEN: BEPLAD
Global Impact Factor 0.876
Universal Impact Factor 0.9804
NAAS Rating 4.95

ORIGINAL ARTICLE **OPEN ACCESS**

Application of $LaNiMnO_6$ perovskite Nanoparticles fabricated on Carboxymethyl Cellulose Microspheres for adsorption of monocrotophos from aqueous environment

Sahithya K*
Department of Microbiology, Karpagam Academy of Higher Education, Coimbatore- 641021, India
*Corresponding author's Email: sahikandimalla@gmail.com

ABSTRACT

Effective removal of organic pollutants from aqueous environment by using nanoparticles has become a hot research in recent years. Herein, $LaNiMnO_6$ perovskite (Prv) nanoparticles were synthesized by reverse micro-emulsion method and fabricated on carboxymethyl cellulose (CMC) microspheres to enhance their adsorption activity against organophosphate pesticide, monocrotophos (MCP). The structural, optical and morphological properties of $LaNiMnO_6$ perovskite nanoparticles were studied by using Scanning Electron Microscopy (SEM), Energy Dispersive X-Ray Spectroscopy (EDX) while Fourier Transform Infrared Spectroscopy (FT-IR) have been used to study the involvement of functional groups during MCP adsorption. The influence of various factors including pH (3.0-12.0), contact time (30-420 min), temperature (20-40 °C), initial MCP concentration (20-140 mg L^{-1}) and dosage (0.4-2.0 g L^{-1}) affecting the adsorption efficiency were also investigated. Adsorption efficiency of CMCPrv and Prv against MCP was found to be 88.3 % and 76.1 % respectively in batch studies. The mechanism of MCP adsorption onto adsorbents was studied using various equilibrium and kinetic models. CMCPrv exhibited a good stability over repeated cycles of pesticide adsorption, which probe the applicability of adsorbent in the treatment of wastewater. The exceptional structural features of $LaNiMnO_6$ perovskite nanoparticles and functional groups of CMC allowed achieving the maximum adsorption of pesticide.

***Key words**: Adsorption, Carboxymethyl cellulose, Monocrotophos, $LaNiMnO_6$ Perovskite nanoparticles, Regeneration studies.*

Received 15.01.2020 Revised 21.02.2020 Accepted 09.03.2020

INTRODUCTION

Extensive use of pesticides to protect crops has been reported to result in the significant transfer of these compounds into the atmosphere and their transmission into freshwater as well as bottled drinking mineral water [1]. Monocrotophos (MCP, CAS number 6923-22-4), one of the highest consumed pesticides in India identified as endocrine disrupting agent that disrupts the endocrine functions such as growth, development and reproduction in animals whose residues are commonly found in not only in vegetables and fruits but more alarmingly in human breast milk [1,2]. MCP has been reported to affect non-target organisms including human beings, bees, birds and fishes [3,4]. Cases of human poisoning are characterized by profuse perspiration, muscular weakness, blurred vision, confusion, vomiting, pain and small pupils. The risk of death due to respiratory failure was also well documented [5]. The prolong use of MCP has found its way into the waterways and recent reports have highlighted the existence of MCP with concentration of 4 µg/L in rain water [6,7].

Effective techniques for the remediation of toxic organic compounds from aqueous environment have drawn significant interest. Adsorption by solid materials shows potential as one of the most efficient methods for the treatment and removal of pollutants in the treatment of industrial wastewater [8].

Double perovskites oxide nanoparticles (Prv) with general formula $A_2B'B''O_6$ have emerged as an important class of nanomaterials in the elimination of various organic and inorganic environmental pollutants due to their nano size, high surface area, stable electronic structure, ionic conductivity, thermal, optical and catalytic properties [9-14].

Carboxymethyl cellulose (CMC) is an ionic polysaccharide, rich in polar carboxyl groups. CMC is regarded to be cheap, abundant, chemical reactivity, biodegradability and strongly chelating properties made CMC as attractive starting material for the remediation of various organic pollutants [15,16].
The present study is the first attempt to investigate the efficiency of perovskite nanoparticles (Prv) fabricated on CMC for removal of MCP from aqueous environment.

MATERIALS AND METHODS

Materials

Monocrotophos (MCP, purity 99.9 %), carboxymethyl cellulose (CMC) and 1-butanol were purchased from Sigma Aldrich Chemicals Co. (USA). Cetyl trimethyl ammonium bromide (CTAB), cyclohexane, lanthanum chloride hexahydrate ($LaCl_3.6H_2O$), nickel nitrate ($Ni(NO_3)_2$), manganese nitrate ($Mn(NO_3)_2$) and acetonitrile were purchased from Sisco Research Laboratories, India.

Synthesis and characterization of adsorbents

The synthesis and characterization of $LaNiMnO_6$ perovskite (Prv) nanoparticles and Prv nanoparticles fabricated on carboxymethyl cellulose (CMCPrv) have been reported in our earlier study [17].

Adsorption studies

Adsorption experiments were conducted in a batch mode under dark conditions using mechanical shaker. The MCP solutions with initial concentration from 20 to 140 mg L^{-1} were agitated with 100 mg of the adsorbent. During the adsorption, 5 mL of the sample was collected every 15 min and centrifuged and the residual concentration of MCP was determined by high performance liquid chromatography (HPLC, Perkin Elmer 200 Series) at 232 nm. The influence of operating parameters *viz*., pH (3.0-12.0), contact time (30-420 min), initial MCP concentration (20-140 mg L^{-1}), temperature (20-50 °C) and dosage (0.4-2.0 g L^{-1}) were studied. All determinations performed in triplicates and results are reported as average. The amount of MCP adsorbed on the adsorbent at a given time, t (min) as calculated from the following equation:

$$R(\%) = \frac{C_0 - C_t}{C_t} \times 100$$

where C_0 is the initial concentration of MCP and C_t is the concentration of MCP at time '*t*' (min).

Equilibrium, kinetic and thermodynamic studies

The equilibrium data of adsorption was analysed using adsorption isotherm models with two parameter equations- Langmuir, Freundlich and Dubinin-Radushkevich (D-R). Pseudo-first order, pseudo-second order, intra-particle diffusion model and Boyd plot have been used for modelling the kinetic data for adsorption of MCP onto adsorbents. The standard free energy (ΔG°), enthalpy (ΔH°) and entropy (ΔS°), for the adsorption process were obtained from the experiments carried out at different temperatures using the standard equations.

Spectroscopic analysis

FT-IR spectra of adsorbents before and after MCP adsorption were recorded on a Jasco FT-IR 4100 spectrophotometer. The changes in surface morphology and the surface elemental composition of adsorbents before and after adsorption of MCP were studied by SEM (Stereo Scan LEO, Model-400) equipped with EDX Microanalysis System (Thermo Electron Corporation, Japan) attached to SEM.

RESULTS AND DISCUSSION

Effect of parameters on adsorption of MCP

The initial solution pH exhibits profound influence on the ionisation of adsorbents and dissociation of pesticides. The effect of initial pH on the adsorption of MCP was studied in the range of 3.0 to 12.0. As shown in Fig. 1(a), maximum adsorption of MCP as observed at pH 6.0 for both CMCPrv and Prv. This could be attributed to the fact that at pH values more than 4.4, MCP is negatively charged which results in higher adsorption by the positively charged CMCPrv (pH_{PZC} - 6.2) and Prv (pH_{PZC} – 7.1). The mutual repulsion between adsorbents and MCP ions decreased the adsorption above pH 7.0 [18]. The influence of contact time on percentage removal of MCP was examined in the range of 30 min to 420 min as shown in Fig. 1(b). The adsorption efficiency of Prv and CMCPrv increased from 21.2 % and 44.8 %, to 55.4 % and 66.7 % when the contact time increased from 30 min to 180 min and 90 min respectively. Higher availability of active adsorption sites on CMCPrv and Prv resulted in the rapid removal at the beginning of adsorption process whereas, no improvement was observed after180 min of contact time due to the saturation of active sites on the surface of the CMCPrv and Prv [19]. The effect of temperature on the adsorption of MCP, shown in Fig. 1(c), exhibited the maximum adsorption at 30 °C for both CMCPrv and Prv du to the increased solubility of pesticides [20]. The effect of initial MCP concentration on the

adsorption is presented in Fig. 1(d). An increase in the removal was noted with the increase in the initial MCP concentration up to 120 mg L^{-1} for CMCPrv and 60 mg L^{-1} for Prv. The competitiveness between the MCP molecules may be attributed for the lower adsorption in the later stages [21]. The dependence of MCP removal on the dosage of CMCPrv and Prv was studied by varying the adsorbent dosage from 0.4 mg L^{-1} to 2 mg L^{-1} while maintaining remaining optimum parameters. As shown in Fig. 1(e), the percentage of adsorption was increased evidently with the increase in adsorbent dosage from 0.4 mg L^{-1} to 0.8 mg L^{-1} for CMCPrv and 1.2 mg L^{-1} for Prv could be explained on the basis of availability of higher number active sites [22]. Therefore, maximum removal of MCP by CMCPrv and Prv was found to be 88.3 % and 76.1 % respectively under optimized conditions.

Equilibrium, kinetic and thermodynamic studies

Table 1 represents isotherm and kinetic constants, correlation coefficient values (R^2) and error values (SSE, SE, RMSE and APE). Among the two parameter isotherms used, Freundlich isotherm was found to exhibit the best fit with the low error (APE) values and high correlation (R^2) values which suggested a heterogenous mode of adsorption of MCP onto Prv and CMCPrv [22]. The uptake value was noted to be higher in case of CMCPrv compared to Prv with higher K_F values. The experimental data of the present study also suggested Langmuir and D-R model showed a poor fit with high APE values and low R^2 values (Fig. 2a).

Of the various kinetic models tested, pseudo-first order showed the best fit as compared to pseudo second order with high R^2 values and low APE values [23]. The suitability of pseudo-first order further suggested the involvement of physical forces in the adsorption of MCP (Fig. 2b). The kinetic data was further analysed by intra-particle diffusion and Boyd plot to check whether the adsorption proceeds via film diffusion or intraparticle diffusion mechanism. As shown in Fig. 1 (c-d), the plots were linear but nor passed through the origin which clearly suggested the both intra-particle and film diffusion played a significant role in the adsorption of MCP on to adsorbents.

The thermodynamic parameters, the standard Gibbs energy change, ΔG°, the standard enthalpy change, ΔH° and the standard entropy change, ΔS°, were calculated using the experimental data obtained at various temperatures and tabulated (Table 2). The negative values of ΔG° at various temperatures indicated the spontaneous nature of the MCP adsorption from aqueous solutions by both the adsorbents. The positive values of ΔH° reflected the endothermic nature of the adsorption. The positive values of ΔS° suggested an increased randomness at the solid/liquid interface during the MCP adsorption on the CMCPrv and Prv.

Spectroscopic studies

Fig. 3 displays the FT-IR spectra of Prv and CMCPrv before and after adsorption of MCP. The stretches at 3344.57 cm^{-1} suggested the role of primary amines in the adsorption of MCP by CMCPrv (Fig. 3d). The peaks at 2920.23 cm^{-1}, 2852.72 cm^{-1} and 524.64 cm^{-1} in case of CMCPrv corresponds to the stretching and bending vibrations of C=O and H-O-C=O which revealed involvement of carboxylic acids in the adsorption of MCP molecules (Fig. 3d). The presence of -P-O phosphate groups (1085.21 cm^{-1} and 1053.13 cm^{-1}) in both Prv and CMCPrv spectrum confirmed the adsorption of MCP molecules (Fig. 3c-d). Maximum transmittance was noted in case of CMCPrv which suggested their major involvement in the adsorption process.

The morphological changes on the surface of CMCPrv before and after adsorption of MCP were studied by using scanning electron microscope (Fig. 4). A uniform distribution of perovskite nanoparticles on the surface of CMCPrv improved the surface roughness which further contributed in high adsorption of MCP molecules.

EDX studies were performed for identification of major elements present in the CMCPrv before and after adsorption. As shown in Fig 5a, Carbon (C), Nickel (Ni), Lanthanum (La) and Manganese (Mn) ions were the predominant metal species present on the surface of CMCPrv. The presence of P peak after the adsorption of MCP confirmed the adsorption of MCP onto CMCPrv (Fig. 5b). Moreover, a significant decrease in C peak suggested the involvement of C containing functional groups of CMC in adsorption of MCP which further favoured the maximum MCP adsorption.

Regeneration studies

Recyclability and stability of adsorbent is a key feature for analyzing their potential applicability for industrial applications and for the development of efficient adsorbent for waste water treatment. To determine the reusability of the CMCPrv adsorbent, experiments were repeated up to six cycles. After every reaction the CMCPrv was separated by centrifugation, washed and dried at 70 °C and then reused without any further treatment. The same procedure was employed for all the successive cycles. As shown in Fig. 6, it was observed that the removal efficiency of CMCPrv adsorbent remained almost constant for

the first three cycles whereas, a decrease in percentage adsorption was noticed for successive cycles which could be due to the loss of active sites.

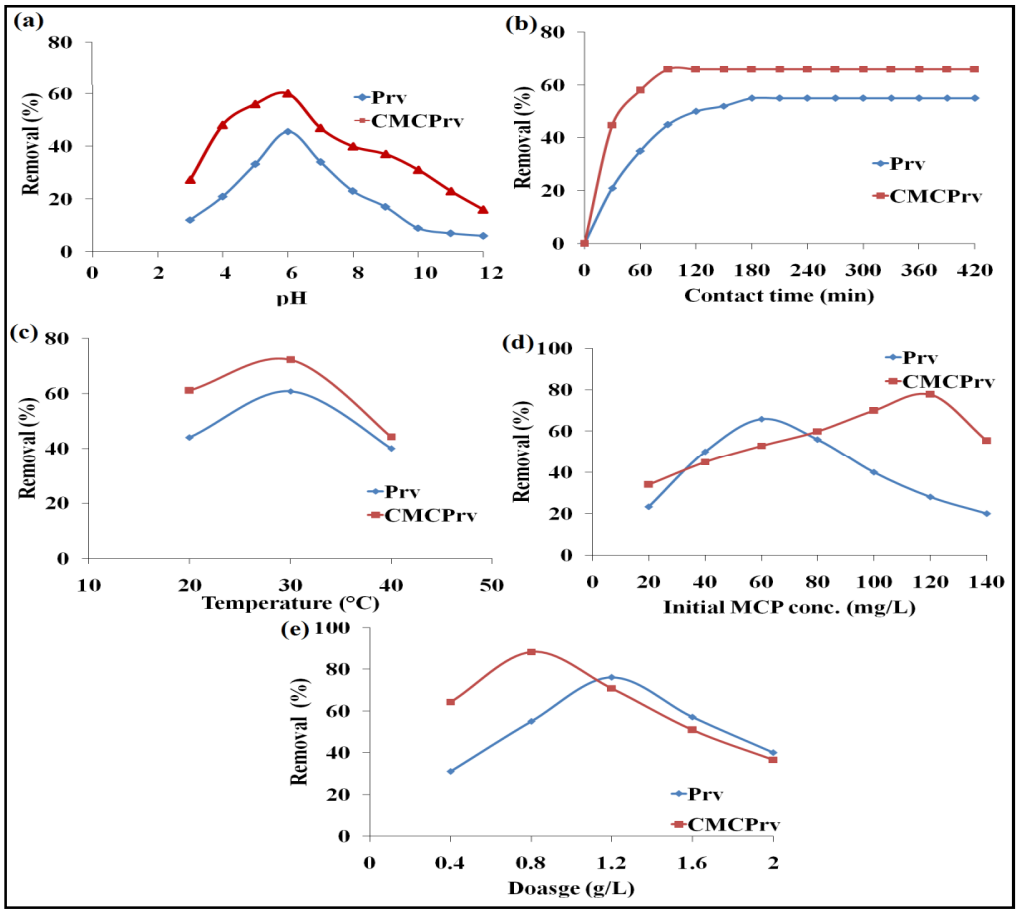

Fig. 1 Effect of parameters on adsorption of MCP by Prv and CMCPrv. (a) pH (b) contact time (c) temperature (d) initial MCP concentration and (e) dosage

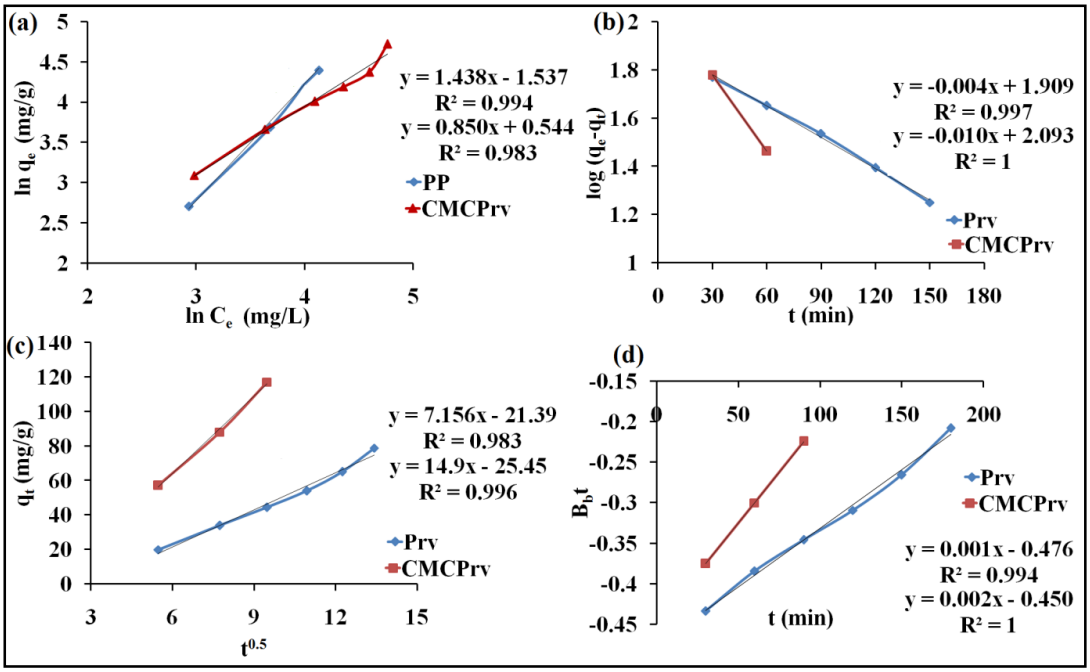

Fig. 2. (a) Freundlich isotherm (b) Pseudo-first order (c) Intraparticle diffusion and (d) Boyd plot of MCP adsorption onto Prv and CMCPrv.

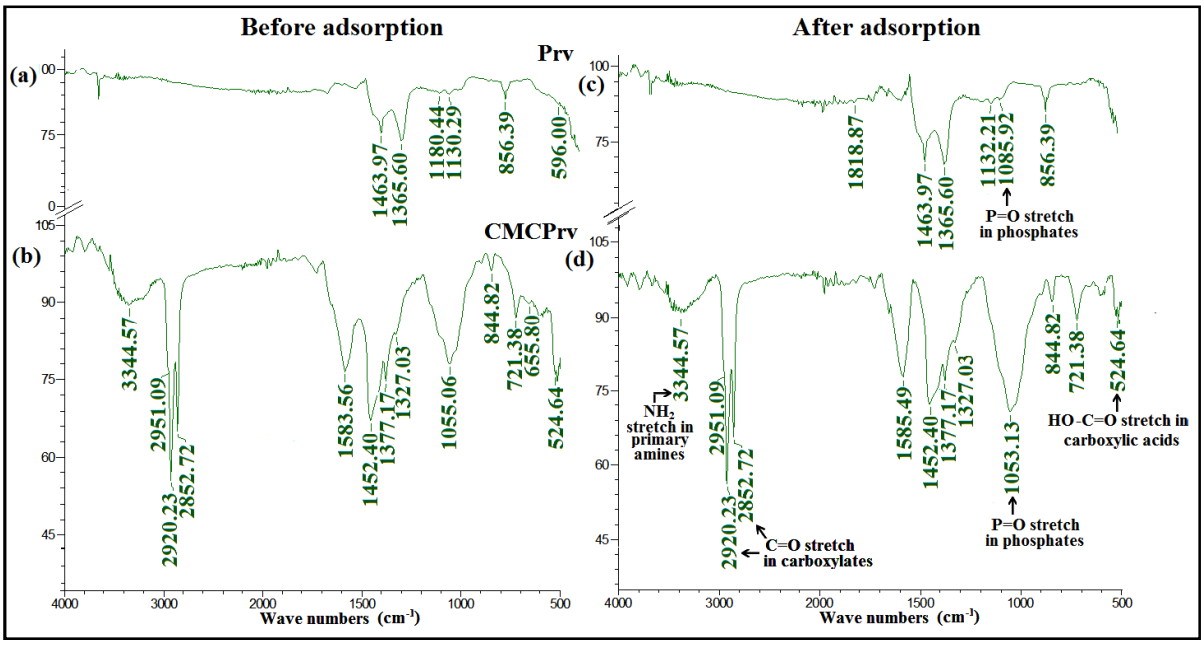

Fig. 3. FT-IR spectra of Prv and CMCPrv before (a, b) and after (c, d) MCP adsorption

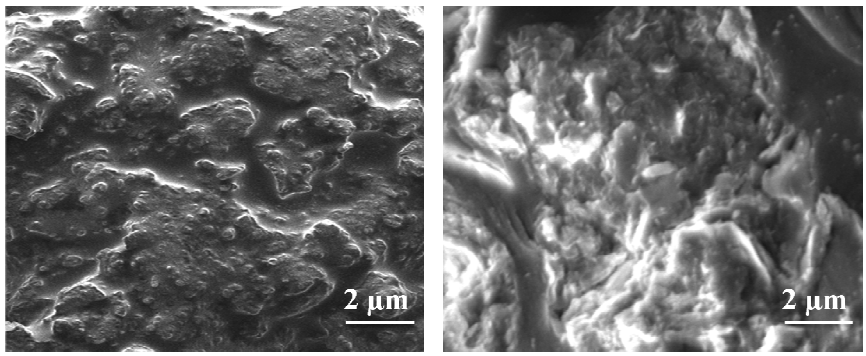

Fig. 4. Surface morphology of CMCPrv (a) before and (b) after MCP adsorption

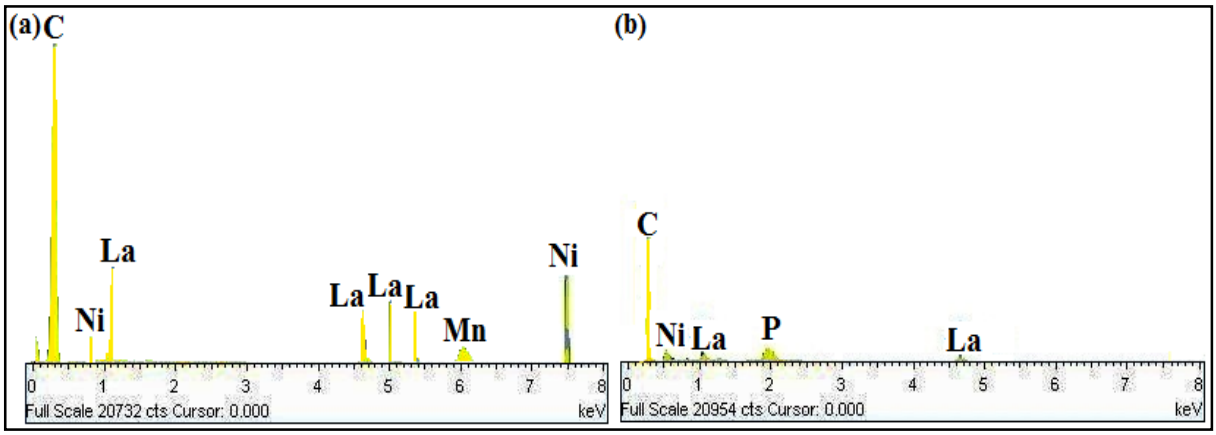

Fig. 5. EDX spectra of CMCPrv (a) before and (b) after MCP adsorption

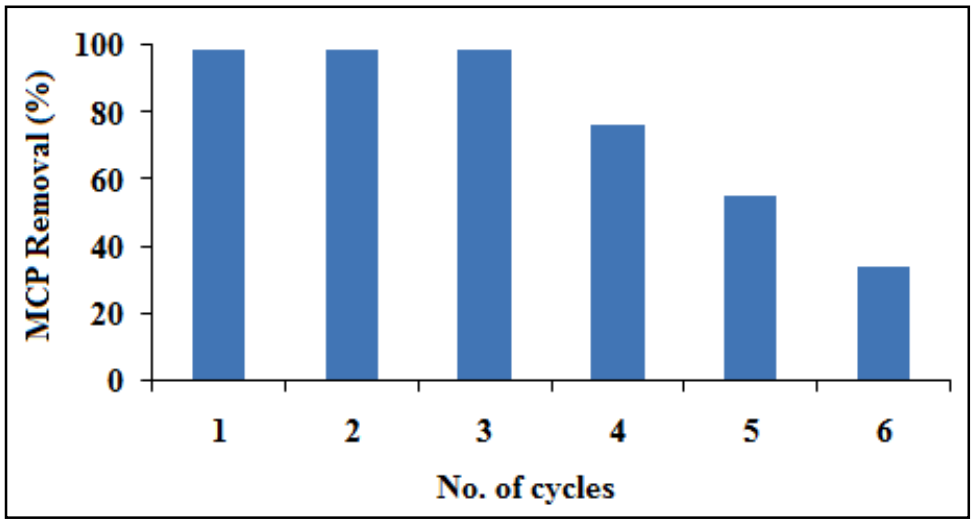

Fig. 6. MCP adsorption as a function of the number of cycles for CMCPrv

Table 1 Equilibrium isotherm and kinetic model parameters for MCP adsorption

Models	Parameters	Prv	CMCPrv
Langmuir	q_m (mg g^{-1})	83.3	125.0
	K_L (L mg^{-1})	0.020	0.009
	R^2	1.00	0.99
	APE (%)	31.04	21.57
Freundlich	n	1.69	1.17
	K_F (mg g^{-1})	4.65	1.72
	R^2	0.99	0.98
	APE (%)	28.2	4.74
D-R	q_m (mg g^{-1})	84.9	121.5
	E (KJ mol^{-1})	0.22	0.15
	β (mol^2 J^{-2})	$1*10^{-5}$	$2*10^{-5}$
	R^2	0.98	0.96
	APE (%)	28.81	10.1
Pseudo first order	q_e	81.09	125.8
	K_1 (min^{-1})	0.009	0.02
	R^2	0.99	1.00
	APE (%)	2.18	3.79
Pseudo second order	q_e	83.3	111.1
	K_2 (g mg^{-1} min^{-1})	$5*10^{-4}$	$1*10^{-3}$
	R^2	0.98	0.99
	APE (%)	27.6	18.6
Intra-particle diffusion	V	7.15	14.9
	C	21.3	25.4
	R^2	0.98	0.99
	APE (%)	4.73	1.52

Table 3 Thermodynamic parameters of MCP adsorption

Adsorbent	Temperature (K)	ΔH° (KJ mol^{-1})	ΔS° (KJ mol^{-1} K^{-1})	ΔG° (KJ mol^{-1})
Prv	283	+17.5	+0.06	+0.59
	293			-0.01
	303			-0.61
CMCPrv	283	+21.9	+0.08	-0.74
	293			-1.54
	303			-2.34

CONCLUSION

The adsorptive removal of MCP using $LaNiMnO_6$ perovskite nanoparticles (Prv) has been investigated. A significant increase in removal was noted when Prv nanoparticles fabricated on carboxymethyl cellulose

(CMCPrv). The most efficient equation for describing the isotherms was Freundlich model exhibiting the heterogenous mode of MCP adsorption by both Prv and CMCPrv which was confirmed by SEM analysis. Kinetic studies on adsorption of MCP on adsorbents revealed that pseudo first order model showed the best fit to the experimental data and intra-particle, and film diffusion were involved in the adsorption process. FT-IR analysis suggested that carbonyl (C=O) and carboxyl (-COOH) groups are mainly involved in MCP uptake by Prv and CMCPrv. Application of CMCPrv could serve as an effective remediation tool for the treatment of wastewater containing MCP.

ACKNOWLEDGEMENT

We take this opportunity to thank VIT University, Vellore and SAIF-IIT, Bombay who helped us for the instrumental analysis.

REFERENCES

1. Nagaraju, R. & Rajini, P.S. (2016). Adaptive response of rat pancreatic β-cells to insulin resistance induced by monocrotophos: Biochemical evidence. Pestic. Biochem. Phys. 134:39-48.
2. Salim, C., Nidheesh, T., Muralidhara, M. & Rajini, P.S. (2018). Insights on the age dependent neurodegeneration induced by Monocrotophos, (an organophosphorous insecticide) in *Caenorhabditis elegans* fed high glucose: Evidence in wild and transgenic strains. Comp. Biochem. Phys. C. 211:15-24.
3. Nidheesha, T., Salima, C., Rajinia, P.S. & Suresh, PV. (2016). Antioxidant and neuroprotective potential of chitooligomers in *Caenorhabditis elegans* exposed to Monocrotophos. Carbohydr. Polym. 135:138–144.
4. Jaiswal, D.K., Verma, J.P., Krishna, R., Gaurav, A.K. & Yadav J. (2019). Molecular characterization of monocrotophos and chlorpyrifos tolerant bacterial strain for enhancing seed germination of vegetable crops. Chemosphere 223:636-650.
5. Kaur, R. & Goyal, D. (2019). Toxicity and degradation of the insecticide monocrotophos. Environ. Chem. Lett. DOI: 10.1007/s10311-019-00884-y
6. Bhalerao, T.S. & Puranik, P.R. (2009). Microbial degradation of monocrotophos by *Aspergillus oryzae.* Int. Biodeter. Biodegr. 63:503-508.
7. Zhang, X., Tian, H., Wang, W. & Ru S. (2013). Exposure to monocrotophos pesticide causes disruption of the hypothalamic-pituitary-thyroid axis in adult male gold fish (*Carassius auratus*). Gener. Compar. Endocrinol. 193:158-166.
8. Girish, C. R. (2018). Simultaneous adsorption of pollutants onto the adsorbent review of interaction mechanism between the pollutants and the adsorbent. International J. Eng. Techno. 7(4),3613-3622
9. Thirumalairajan, S., Girija, K., Ganesh, I., Mangalraj, D., Vishwanathan, C., Balamurugan, N. & Ponpandian, N. (2012). Controlled synthesis of perovskite $LaFeO_3$ microsphere composed of nanoparticles via self-assembly process and their associated photocatalytic activity. Chem. Eng. J. 209:420-428.
10. Tavakkoli, H. & Yazdanbakshsh, M. (2013). Fabrication of two Prv type oxide nanoparticles as the new adsorbents in efficient removal of a pesticide from aqueous solution: Kinetic, thermodynamic and adsorption studies. Mesopor. Micropor. Mater. 176:86-94.
11. Areqi, N.A.S.A., Alas, A.A., Kamali, A.S.N.A., Ghaleb, K.A.S. & Mureish, K.A. (2014). Photodegradation of 4-SPPN dye catalyzed by Ni(II)-substituted $Bi_2VO_{5.5}$ system under visible light irradiation: Influence of phase stability and Prv vanadate-oxygen vacancies of photocatalyst, J. Molecular Cataly A: Chemical, 381:1-8.
12. Labhasetwar, N., Saravanan, G., Megarajan, S.K., Manwar, N., Khobragade, R., Doggali, P. & Grasset, F. (2015). Perovskite-type catalytic materials for environmental applications, Sci. Technol. Adv. Mater. 16(3):036002.
13. Vasala, S. & Karppinen, M. (2015). $A_2B'B''O_6$ perovskites: A review. Progr. Solid. State. Chem. 43:1-36.
14. Zhu, H., Zhang, P. & Dai, S. (2015). Recent advances of lanthanum-based perovskite oxides for catalysis. ACS Catal. 5:6370-6385.
15. Nádia, S.V.C., Mansur, A.A.P., Mansur, H.S., Jesus, A.C., Carvalho, S.M., Chagas P. & Oliveira, L.C. (2018). Eco-friendly and biocompatible cross-linked carboxymethylcellulose hydrogels as adsorbents for the removal of organic dye pollutants for environmental applications, Environ. Techno. 39(22)2856-2872.
16. Nelson, R.V., Davila, R.A.E. & Sumalapao, D.E.P. (2018). Removal of Lead (II) by Lumbang, Aleurites moluccana Activated Carbon Carboxymethyl cellulose Composite Crosslinked with Epichlorohydrin. Orien. J. Chem. 34(2):693-703.
17. Sahithya, K., Das, D., & Das, N. (2017). Adsorption coupled photocatalytic degradation of dichlorvos using $LaNiMn_{06}$ perovskite nanoparticles supported on polypropylene filter cloth and carboxymethyl cellulose Microspheres, Environmental Progress & Sustainable Energy, 36(1):180-191.
18. Mohammad M & Mohammad R.H. (2018). Reactive orange 16 dye adsorption from aqueous solutions by psyllium seed powder as a low-cost biosorbent: kinetic and equilibrium studies. Appl. Water. Sci 8:212-220.
19. Gholamreza, M., Hiwa, H. & Ahmad, A. (2013). The investigation of diazinon pesticide removal from contaminated water by adsorption onto NH4Cl-induced activated carbon. Chem. Eng. J. 214:172-179.
20. Sabino, D.G., Lofrano, G., Mariangela, G. & Michele, N. (2016). Characteristics and adsorption capacities of low-cost sorbents for wastewater treatment: A review. Sustain. Mater. Techno. 9:10-40.
21. Aparajita, S., Manasa, K., Vipin, K.S. & Amit, K. (2020). Removal of pentachlorophenol pesticide from aqueous solutions using modified chitosan. Arab. J. Chem. 13(1):1821-1830

22. Smedt, C.D., Ferrer, F., Leus, K. & Spanoghe, P. (2015). Removal of Pesticides from Aqueous Solutions by Adsorption on Zeolites as Solid Adsorbents. Adsorption. Sci. Technol. 33(5):457-485.
23. Chattoraj, S., Mondal, N.K. & Sen, K. (2018). Removal of carbaryl insecticide from aqueous solution using eggshell powder: a modeling study. Appl. Water. Sci. 8:163-171.
24. Chattoraj, S., Mondal, N.K., Sadhukhan, B., Bikash, S., Palas, R. & Tapas, K. (2016). Optimization of Adsorption Parameters for Removal of Carbaryl Insecticide Using Neem Bark Dust by Response Surface Methodology. Water. Conserv. Sci. Eng. 1:127–141.

CITATION OF THIS ARTICLE

Sahithya K. Application of $LaNiMnO_6$ perovskite Nanoparticles fabricated on Carboxymethyl Cellulose Microspheres for adsorption of monocrotophos from aqueous environment. Bull. Env. Pharmacol. Life Sci., Vol 9[4] March 2020: 66-73